

Recent substantial changes in Bering Sea ice area

by Gerd Wendler & Telayna Wong¹

Abstract: In the present study, we analyzed the sea ice area of the Bering Sea, the ocean between Siberia and Alaska. Understanding the trends in Bering Sea ice area is especially important for fisheries, as it is the most productive of all coastal waters of North America. Here, sea ice is typically formed in October, grows rapidly in November, and reaches its maximum amount in March. It melts in June, leaving the late summer/early autumn (July – October) mostly ice free. Interestingly, in contrast to the Northern Hemisphere at large, including the Chukchi and Beaufort Seas, there was no observed systematic decrease in the amount of Bering Sea ice for the 38 year time period (1979-2017), for which there are reliable satellite data. Interestingly, both the absolute minimum as well as absolute maximum in the sea ice area was observed in the last six years of the time period under examination. The variations in sea ice area of the Bering Sea are well correlated with the annual PDO (Pacific Decadal Oscillation) values, which are deduced from the water temperature in the Pacific Ocean north of 20°N. The PDO is related to the El Niño 3.4, and both are strongly related to the amount of sea ice in the Bering Sea.

Zusammenfassung: In der vorliegenden Studie haben wir Schwankungen der Meereisverbreitung im zwischen Sibirien und Alaska gelegenen Beringmeer analysiert. Das Verständnis der Meereis-Trends ist für die Fischerei besonders wichtig, da das Beringmeer das produktivste aller Küstengewässer Nordamerikas darstellt. Dort bildet sich Meereis in der Regel im Oktober, wächst im November schnell an und erreicht im März seine maximale Verbreitung. Es schmilzt im Juni und hinterlässt im Spätsommer und Frühherbst (Juli – Oktober) ein weitgehend eisfreies Areal. Im Gegensatz zum gesamten Arktischen Ozean, einschließlich der Tschuktschensee und der Beaufortsee, wurde im Zeitraum von 38 Jahren (1979-2017), für den zuverlässige Satellitendaten vorliegen, kein systematischer Rückgang der Meereisverbreitung im Beringmeer beobachtet. Sowohl das absolute Minimum als auch das absolute Maximum der Meereisverbreitung wurden in den letzten sechs Jahren des Untersuchungszeitraums beobachtet. Die Schwankungen der Meereisfläche des Beringmeeres korrelieren gut mit den jährlichen Werten der Pazifischen Dekaden-Oszillation (PDO), die von der Wassertemperatur im Pazifik nördlich von 20°N abgeleitet werden. Die PDO ist mit der El-Niño-3.4-Oszillation verwandt, und beide sind offenbar stark mit der Meereismenge im Beringmeer verknüpft.

INTRODUCTION

The Bering Sea (Fig. 1) is a marginal sea of the Pacific Ocean that is separated from the Gulf of Alaska by the Alaska Peninsula and from the Chukchi Sea by the Seward Peninsula. It extends over two million square kilometres and is bordered by Alaska to the east and southeast, by Russia and the Kamchatka Peninsula to the west, by the Alaska Peninsula and the Aleutian Islands to the south, and on the far north by the Bering Strait, which connects the Bering Sea and the Chukchi Sea. The Bering Sea is named for Vitus Bering, who in 1728, was the first person to carefully explore it from its edge in the Pacific Ocean northward. At this time, Alaska was a part of the Russian empire. The Yukon River, originating in Canada and flowing across Alaska, is a major source of fresh water for the Bering Sea.

Keywords: Bering Sea, climate variations, sea ice area, Pacific Decadal Oscillation (PDO)

Schlüsselwörter: Beringmeer, Klimaschwankungen, Meereisverbreitung, Pazifische Dekaden-Oszillation

doi:10.2312/polarforschung.88.2.151

¹ Alaska Climate Research Center, Geophysical Institute, University of Alaska
Manuskript eingereicht 6. August 2019; zum Druck angenommen 16. August 2019

SEA ICE DATA SOURCES

Sea ice observations of the Arctic Ocean go back to the 19th century, with the early ones carried out mostly from coastal observations and occasional expeditions into the Arctic Ocean. The United Kingdom Meteorological Office (UKMO 1969) as well as the Danish Meteorological Office (DMI 2012) published maps based on these historical data. Furthermore, WALSH et al. (2017) synthesized observational data from as far back as 1850. In addition to land based observations, in the late 19th century and early 20th century, whaling in the coastal waters of Alaska was a source of additional information on the sea ice condition. However, a reliable trend of the sea ice area cannot be deduced from these data. Satellite images in the visible region became available in the 1960's, but were of limited value due to extensive darkness in winter, inhibiting the ability to distinguish between clouds and sea ice. MCCAIN & BAKER (1969) applied 5-days minimum brightness data to obtain the presence or absence of sea ice. This brightness data method was also applied to the coastal area of the Beaufort Sea (WENDLER 1973). However, the results were somewhat uncertain due to the high amount of cloudiness in the Arctic; if the cloud cover lasted more than five consecutive days, the amount of sea ice was over-estimated. In 1978, reliable satellite data measuring in the microwave spectrum became available, allowing scientists to see sea ice through darkness and clouds (CAVALIERI et al. 2006). The National Snow and Ice Data Center (NSIDC) of the University of Colorado Boulder (FETTERER et al. 2010) offers scanning multi-channel microwave radiometer data from which reliable sea

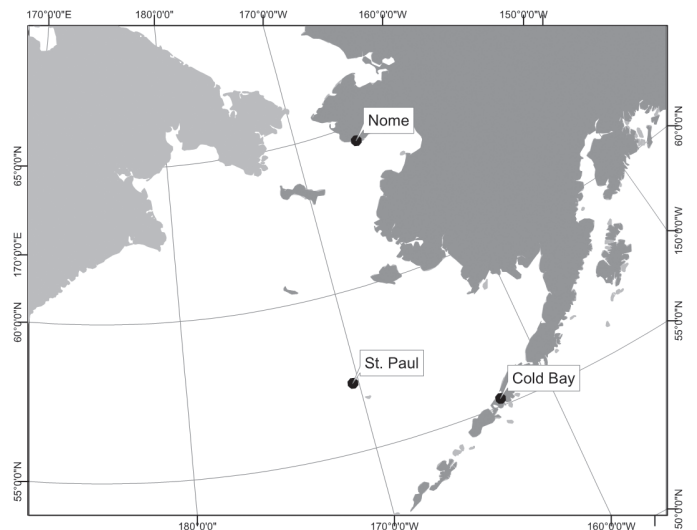


Fig. 1: Map of the Bering Sea identifying the three first order stations analyzed in this study.

Abb. 1: Karte des Beringmeeres mit den drei in dieser Studie analysierten Stationen erster Ordnung.

ice area measurements are obtained. In this study, we utilize NSIDC data to examine maximum, minimum, and average monthly and annual sea ice area data from the Bering Sea and the Northern Hemisphere at large for the time period of 1979-2017. We chose to focus particularly on the average annual sea ice area values, as these are more conservative values for correlating to other meteorological and climatological parameters.

RESULTS

National Snow and Ice Data Center data show that the total amount of sea ice in the Arctic Ocean has decreased. However, the decrease was non-linear, both in time and place. Using the mean of such data for the Northern Hemisphere between 1979 to 2017, the total amount of sea ice decreased from 9.8 to 8.9 million km², or on average, by 0.24% per year. While the changes in the central Arctic Ocean are relatively minor up until now, substantial changes were observed in the more southerly coastal areas of the Arctic Ocean. The Beaufort and the Chukchi Seas, north of the Alaskan coast, reported substantially higher reductions in sea ice (WENDLER et al. 2014b). This reduction is especially pronounced in coastal autumn, allowing for increased summer and autumn navigation in the coastal waters, but contributing to erosion of the coastline due enhanced lack of sea ice to suppress the wave action.

In contrast to the sea ice in the Central Arctic Ocean, where the sea ice does not totally melt in summer, Bering sea ice is seasonal (Fig. 2). July through September is normally ice-free, and ice begins to form in October with the amount increasing until March, when normally the maximum amount for the season is reached. Thereafter, the decrease is substantial, especially in late spring, and by early summer (June), the last sea ice disappears.

Figure 3 shows a time series of the mean annual sea ice area for the Northern Hemisphere and the Bering Sea. The mean annual sea ice area in the Northern Hemisphere has decreased by some 10% over the last four decades. This result is not unexpected due to observed global warming that is especially pronounced in polar regions (SERREZE & BARRY 2006, WALSH & CHAPMAN 1996, WALSH et al. 2017). No mean annual value of sea ice under eight million km² has yet been observed. Interestingly, the decrease in sea ice is hardly visible in the annual maxima.

As these maxima occur in winter, one can deduce that more summer melting must have occurred over the last 39 years. However, the Bering Sea is ice free in summer, and hardly any systematic decrease in the amount of sea ice between 1979 - 2017 could be observed. However, the annual variations from year to year are relatively strongly pronounced and are related to the Pacific Decadal Oscillation (PDO). In 2012, the sea ice maximum of 290,000 km² occurred, while five years later in 2017, the minimum of about 100,000 km² was observed, a value only about a third of the area of the maximum. These large annual variations for the Bering Sea are due to its smaller area and its openness to the Pacific Ocean. The conditions of the Pacific naturally have a strong influence on the formation of the sea ice.

The water temperature of the Northern Pacific Ocean is strongly influenced by the El Nino 3.4, with offshore winds especially pronounced in the coastal area of Northern Chile. Normally, the coastal area sees consistent offshore winds that make the area a semi-desert by causing upwelling of cold water, nutrient-rich water from the bottom layers of the ocean. However, the wind direction sometimes reverses and the "El Nino" phenomenon brings above normal temperatures and much needed rain to the coastal area. This warm surface water is then transported to northern waters. The PDO is

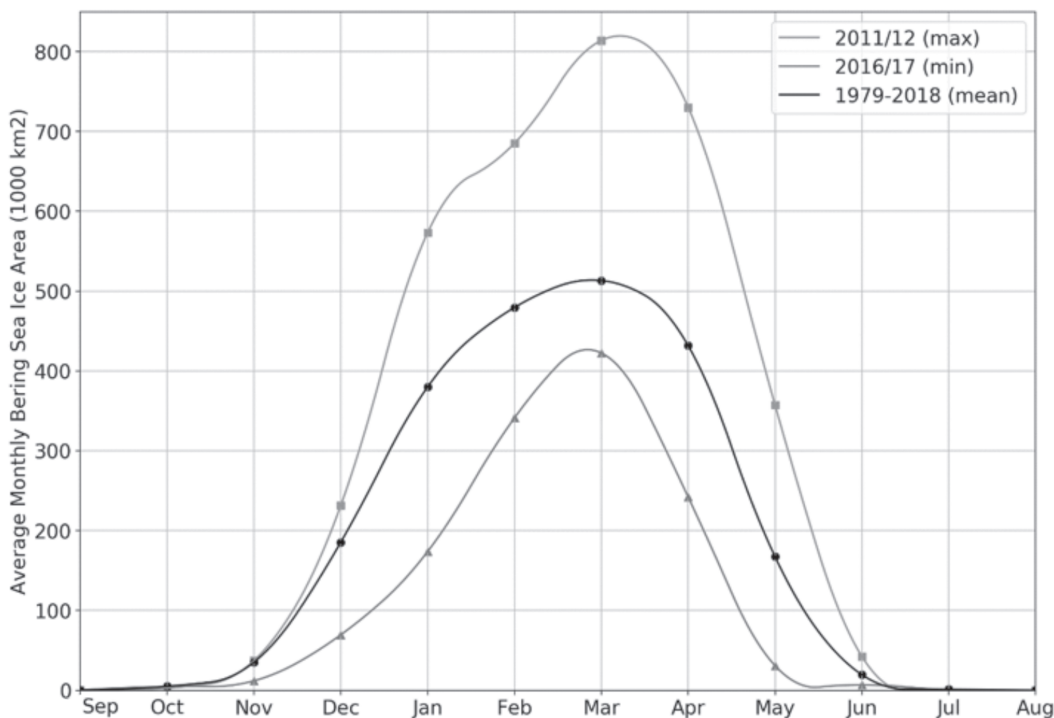


Fig. 2: Annual course of the Bering Sea ice area maximum, minimum, and mean conditions.

Abb. 2: Jährlicher Verlauf der maximalen, minimalen und mittleren Meereisverbreitung im Beringmeer.

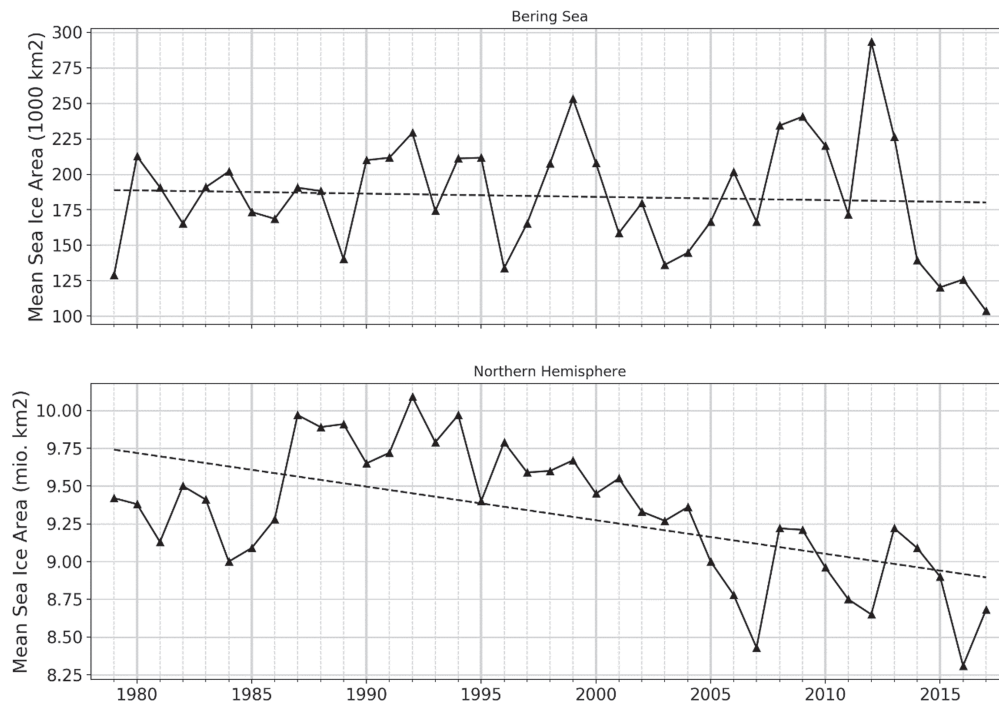


Fig. 3: Time series of the Bering Sea and the Northern Hemisphere mean sea ice area; note the major differences in the y-axis between the graphs due to scale.

Abb. 3: Zeitreihen des Beringmeeres und der nördlichen Hemisphäre bedeckten Meereisfläche. Beachten Sie die großen Unterschiede in der y-Achse zwischen den Diagrammen auf Grund der Skalierung.

related to this phenomenon, and can be derived from the water temperatures of the Pacific Ocean north of 20°N. MANTUA et al. (1997) were the first to show the strong influence of the phase of the PDO on the climate of Alaska, and furthermore, the effect on productivity of fisheries. Positive PDO values reflect above normal temperatures, while negative values represent below normal temperatures. A time series of mean annual PDO values is presented in Figure 4. For the Bering Sea, the maximum sea ice area value was observed in 2012, the year in which the PDO was at its lowest value of -1.5 of

the 38-year time period, while the last four years of strongly positive PDO values in our time series were associated with below normal sea ice area values. Other studies, e.g. PAPINEAU (2001), HARTMANN & WENDLER (2005), have also showed a well-established relationship between the amount of sea ice and PDO value.

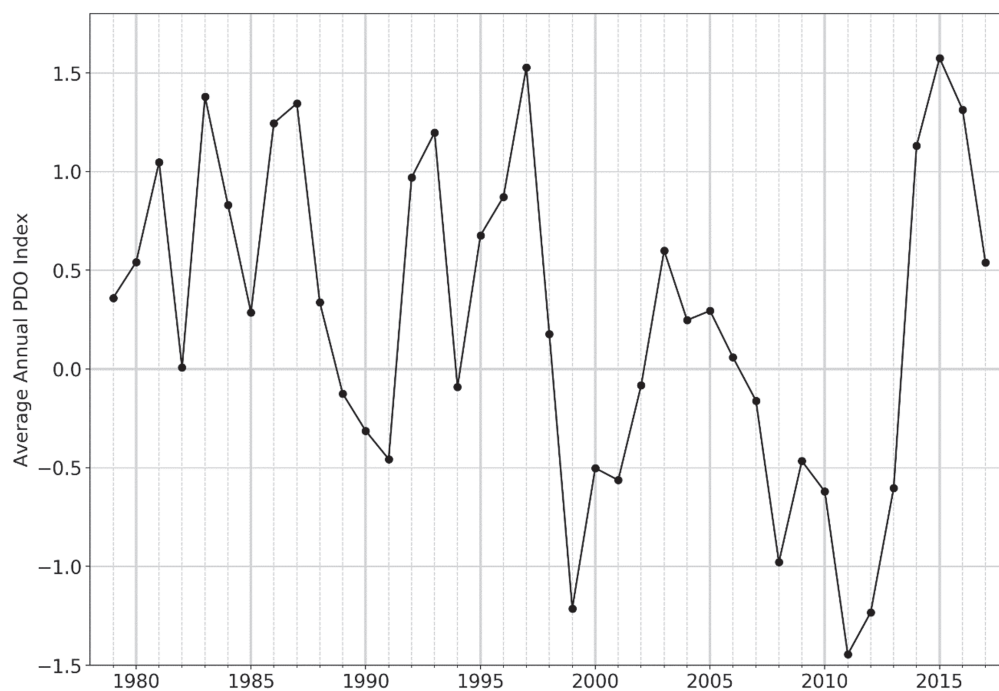


Fig. 4: Time series of mean annual PDO values for 1979-2017.

Abb. 4: Zeitreihen der durchschnittlichen jährlichen PDO-Werte für die Jahre 1979 bis 2017.

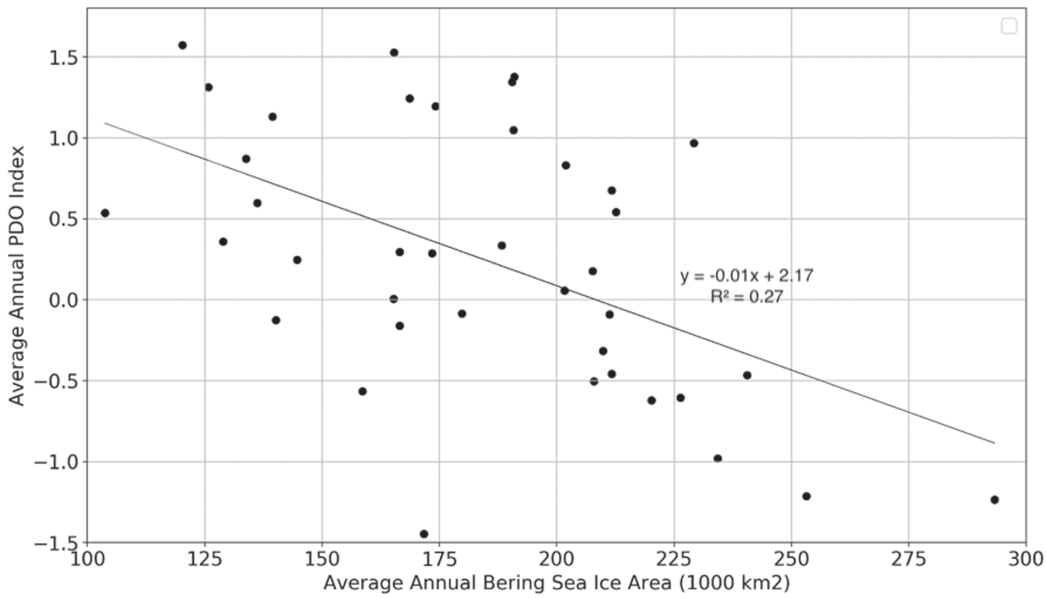


Fig. 5: The relationship between annual values of sea ice area and PDO value.

Abb. 5: Der Zusammenhang zwischen den Jahreswerten der Meereis-ausdehnung und den PDO-Werten.

In Figure 5 we plotted the mean annual PDO value against the mean annual sea ice area of the Bering Sea. While a relationship between negative values of the PDO and increased sea ice area exists, it is not as strong as might be expected, likely because there is no sea ice during the summer months. Positive PDO values in summer correspond to above normal water temperatures, and increased water temperatures negatively impact the formation processes and overall amount of sea ice in autumn, as the water takes more time to cool to the freezing point.

Figure 6 shows a plot of the mean annual air temperatures from three Alaskan coastal stations of the Bering Sea (Nome, St. Paul Island, and Cold Bay) against the annual PDO values for the same years. These three stations were chosen as they are the only available first order stations for this geographic area with a complete series of data. First order stations are operated by the National Weather Service and represent the highest quality weather observations available.

The positions of these stations represent roughly a north-south cross-section of the Bering Sea. Figure 6 shows that the mean annual temperature decreases by some 2°C when going north from Cold Bay to St. Paul Island, and an additional 4°C when going further north to Nome. Furthermore, the dependency of the temperature on the PDO value is also well pronounced and

St. Paul Island, and Cold Bay) against the annual PDO values for the same years. These three stations were chosen as they are the only available first order stations for this geographic area with a complete series of data. First order stations are operated by the National Weather Service and represent the highest quality weather observations available.

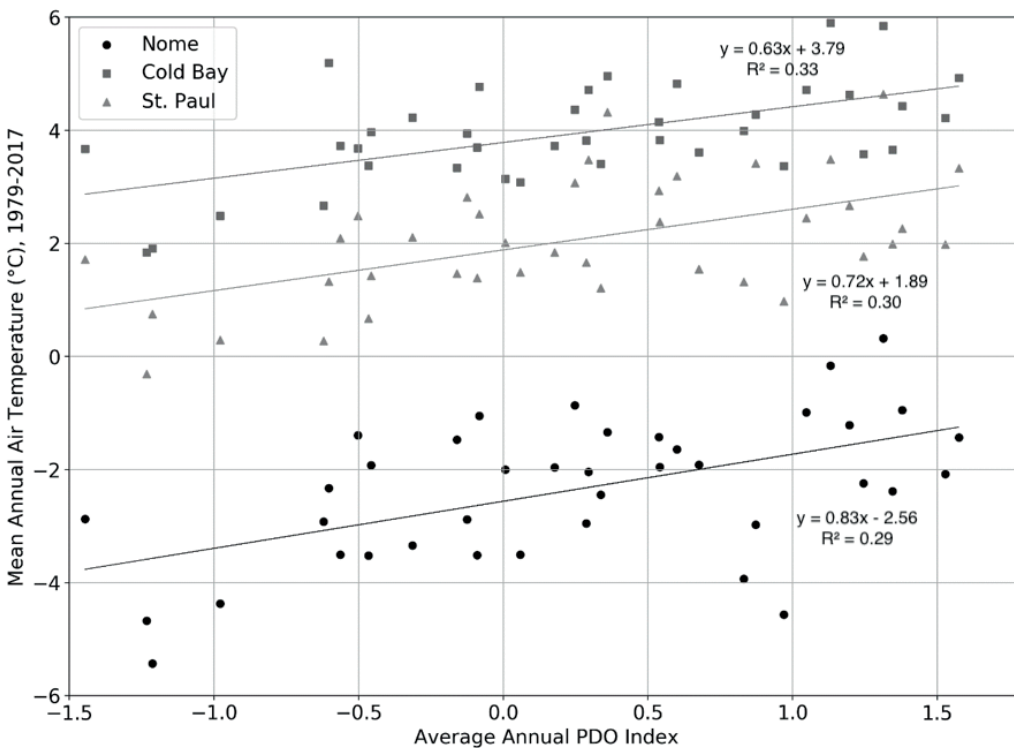


Fig. 6: The mean annual temperature of Cold Bay, St. Paul Island and Nome plotted against the averaged annual PDO index from 1979-2017.

Abb. 6: Die mittlere Jahrestemperatur von Cold Bay, St. Paul Island und Nome, aufgetragen gegen den durchschnittlichen jährlichen PDO-Index für den Zeitraum 1979 bis 2017.

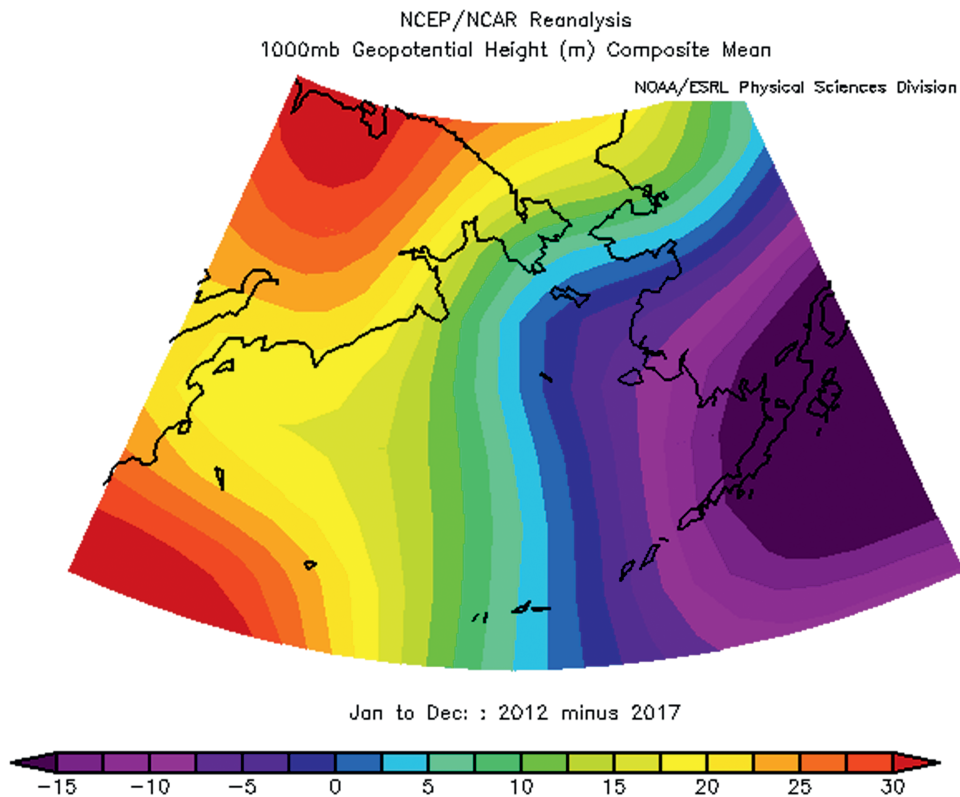


Fig. 7: Difference in the 1000 mb geophysical height between 2012, the year with the greatest Bering Sea ice area, and 2017, the year in our study with the lowest sea ice area, based on the NCEP/NCAR reanalysis of the Bering Sea. NCEP Reanalysis data provided by the NOAA/OAR/ESRL PSD, Boulder, Colorado, USA, from their website at <https://www.esrl.noaa.gov/psd/>.

Abb. 7: Differenz in der geophysikalischen Höhe von 1000 mb zwischen 2012, dem Jahr mit der größten Eisfläche im Beringmeer; und 2017, dem Jahr mit der niedrigsten Meereisfläche im Untersuchungszeitraum; basierend auf der NCEP/NCAR-Reanalyse des Beringmeers. NCEP-Reanalysedaten, die von der PSD NOAA/OAR/ESRL, Boulder, Colorado, USA, auf ihrer Website unter <https://www.esrl.noaa.gov/psd/> bereitgestellt wurden.

quite similar for all three stations, with mean annual temperatures being some 2°C warmer for positive PDO values of 1.5 when compared to negative PDO values of the same magnitude.

Finally, we looked also at the National Centers for Environmental Prediction/National Center for Atmospheric Research [NCEP/NCAR] reanalyzed data set (KALNAY 1969). In Figure 7 we present the difference in the geopotential height between the year in our selected time series with the maximum sea ice area (2012) minus the year with the smallest ice area value (2017). The figure shows a strong pressure gradient across the Bering Sea, with the minimum occurring over southern Alaska, and the maximum over Siberia. This results in an additional northerly wind vector, which in 2012, likely sea ice further south. We intentionally compared annual values as even in the summer, northerly winds advect cold water from the Arctic Ocean through the Bering Strait, while southerly winds bring relatively warm water from the Pacific Ocean into the Bering Sea.

CONCLUSION

With 39 years of passive microwave sensing data, we analyzed the average monthly and annual sea ice area of the Bering Sea, a marginal sea connected to the Arctic Ocean by the Bering Strait. Sea ice was generally present from November to May. Variations in the sea ice area from year to year are large; however, no trend in a reduced ice area over the last 39 years could be observed. This is in contrast to the sea ice area measurements from the greater Northern Hemisphere, where a decrease in ice cover of some 10% was observed for this time

period. An even greater decrease in sea ice can be observed when one looks just at two marginal seas of the Arctic Ocean, the Beaufort and Chukchi Seas, which border the northern coast of Alaska (WENDLER et al. 2014). The reason might be found in that the Bering Sea is open to the influence of the Pacific Ocean. Hence, the ice area of the Bering Sea is strongly dependent on the water temperature of the Pacific Ocean, to the PDO is related.

References

- Cavalieri, D., Parkinson, C., Gloersen, P. & Zwally H. (2006):* Sea ice concentration from Nimbus 7, SMMR and DMSP passive microwave data.- National Snow and Ice Data Center, Boulder, Colorado. Digital media.
- Fetterer, F. (2006):* A selection of documentation related to National Ice Center Sea Ice Charts in Digital Format.- NSIDC Special Report 13, Boulder, Colorado.
- Fetterer, F., Knowles, K., Meier, W.N, Savoie, M. & Windnagel, A.K. (2017):* Updated daily: Sea ice index, version 3. Boulder, Colorado USA.- NSIDC: National Snow and Ice Data Center. doi: <https://doi.org/10.7265/NSK072F8>.
- Hartmann, B. & Wendler, G. (2005):* The significance of the of the 1976 Pacific climate shift on the climatology of Alaska.- *Journal of Climate* 18: 4824-4839.
- Kalnay, E. (1996):* NCEP/NCAR reanalyzed 40 year project.- *BAMS* 77: 437-471.
- Mantua, N., Hare, S., Zhang, Y., Wallace, J. & Francis, R. (1997):* A pacific interdecadal climate oscillation with impacts on salmon production.- *BAMS* 78: 1069-1079.
- McCain E.P. & Baker, D. (1969):* Experimental large-scale snow and ice mapping with composite minimum brightness charts.- ESSA Tech. Mem. NESCTM., 12 pp, Dept. of Comm. Washington D.C.
- Papineau, J. (2001):* Wintertime temperatures.- *Int. J. Climatology* 21: 1577-1592.
- Serreze, M. & Barry, R. (2006):* The Arctic Climate System.- Cambridge University Press, 402pp.
- United Kingdom Meteorological Office (1969):* Sea Ice Charts of Polar Basin, Bracknell, England.

- Walsh, J. & Chapman, W.* (1990): Short-term climate variability in the Arctic.- J of Climate 3: 237-250.
- Walsh J., Fetterer, F., Stewart, S. & Chapman, W.* (2017): A database for depicting Arctic sea ice variations back to 1850.- Geophysical Review 107: 89-107.
- Wendler, G.* (1973): Sea ice observations by means of satellite.- JGR 78(8): 1427-1448.
- Wendler, G, Moore, B. & Galloway, K.* (2014a): Strong temperature increase and shrinking sea ice in Arctic Alaska.- Open Atmospheric Science Journal 8: 7-15.
- Wendler G, Chen, L. & Moore, B.* (2014b): Recent sea ice increase and temperature decrease in the Bering Sea area, Alaska.- Theor. Appl. Climatology 117: 393-398.